

The M Domain of atToc159 Plays an Essential Role in the Import of Proteins into Chloroplasts and Chloroplast Biogenesis*

Received for publication, April 29, 2003, and in revised form, June 17, 2003
Published, JBC Papers in Press, July 9, 2003, DOI 10.1074/jbc.M304457200

Kwang Hee Lee, Soo Jin Kim, Yong Jik Lee, Jing Bo Jin, and Inhwan Hwang‡

From the Center for Plant Intracellular Trafficking and Division of Molecular and Life Sciences,
Pohang University of Science and Technology, Pohang 790-784, Korea

Toc159, a protein located in the outer envelope membrane and the cytosol, is an important component of the receptor complex for nuclear-encoded chloroplast proteins. We investigated the molecular mechanism of protein import into chloroplasts by atToc159 using the *ppi2* mutant, which has a T-DNA insertion at *atToc159*, shows an albino phenotype, and does not survive beyond the seedling stage due to a defect in protein import into chloroplasts. First we established that transiently expressing atToc159 in protoplasts obtained from the white leaf tissues of *ppi2* plants complements the protein import defect into chloroplasts. Using this transient expression approach and a series of deletion mutants, we demonstrated that the C-terminal membrane-anchored (M) domain is targeted to the chloroplast envelope membrane in *ppi2* protoplasts, and is sufficient to complement the defect in protein import. The middle GTPase (G) domain plays an additional critical role in protein import: the atToc159[S/N] and atToc159[D/L] mutants, which have a mutation at the first and second GTP-binding motifs, respectively, do not support protein import into chloroplasts. Leaf cells of transgenic plants expressing the M domain in a *ppi2* background contained nearly fully developed chloroplasts with respect to size and density of thylakoid membranes, and displayed about half as much chlorophyll as wild-type cells. In transgenic plants, the isolated M domain localized to the envelope membrane of chloroplasts but not the cytosol. Based on these results, we propose that the M domain is the minimal structure required to support protein import into chloroplasts, while the G domain plays a regulatory role.

The majority of chloroplast proteins are encoded by the nuclear genome and synthesized in the cytosol. Numerous studies have focused on the molecular mechanism of protein import into chloroplasts (1–8). The *in vitro* import assay system, which utilizes purified chloroplasts and *in vitro*-translated precursor protein, is a crucial tool in these studies (1). These analyses have indicated that the N-terminal transit peptide contains all the necessary information for the translocation of cargo proteins from the cytosol into chloroplasts. It has been proposed that following translation, soluble precursor proteins migrate by diffusion to receptor complexes located on the envelope

membranes of chloroplasts (6, 7, 9). The precursor initially binds to lipids of the outer envelope membrane of the chloroplast (10, 11) and subsequently diffuses to the receptor complex. This allows specific interactions between the transit peptide and receptor complex. The precursor is subsequently translocated through a channel formed by subunits of the receptor complexes (12, 13), followed by cleavage of the transit peptide to produce mature protein within the chloroplast (14).

Components of the import complex, including proteins located at the outer and inner envelope membranes, have been identified and characterized at the molecular level (6, 13). However, the exact roles of these components have not yet been fully elucidated. Toc75 forms a channel at the outer envelope membrane for translocation of chloroplast proteins (15, 16). Toc34 and Toc159 may function as receptor components that bind transit peptides of precursor proteins. Recent studies show that these three Toc proteins form a complex at the outer envelope membrane (17). Another protein component, Toc64, may also bind to the transit peptide at early time points (18). However, the role of this protein needs to be further delineated. Using *ppi2* plants, which do not have functional Toc159, Toc159 has been shown to be essential for protein import into chloroplasts as well as chloroplast biogenesis (8). Chloroplasts in *ppi2* plant cells are in a proplastid state with almost no thylakoid membranes, which gives an albino phenotype to the leaf tissues (8). Toc132 and Toc120, two homologs of Toc159, have been identified in the *Arabidopsis* genome (8). However, these homologs do not complement the loss of Toc159 in *ppi2* plants, implying that these proteins are either not expressed in the same cells or are functionally different from Toc159. *ppi1* plants, which contain a mutation at *Toc34*, also have defective protein import into chloroplasts (19), but in contrast to Toc159, the loss of Toc34 in the *ppi1* plant induces a mild phenotype. This may be due to compensation by the expression of Toc33, a close homolog of Toc34 (20). Toc33/34 and Toc159 contain GTP-binding domains; the GTP-binding domain of Toc159 plays a critical role in its targeting to the outer envelope membrane (21, 22). The GTP-binding domains of Toc159 and Toc34 are proposed to form a heterodimer for facilitating Toc159 targeting (21, 22). In addition to the Toc components, the translocon of inner envelope membrane components (Tic)¹ subunits have been identified, including Tic115, Tic55, and Tic40 (23). However, these proteins are less well characterized with respect to their precise roles in protein import.

To clarify the role of Toc159, we examined whether *Arabidopsis thaliana* Toc159 (*atToc159*) supports protein import into chloroplasts when transiently expressed in *ppi2* protoplasts. The atToc159 protein is composed of three different domains, the N-terminal acidic (A), middle GTPase (G), and C-terminal

* This work was supported by Grant M10116000005-02F0000-00310 from the Creative Research Initiatives Program of the Ministry of Science and Technology (Korea). The costs of publication of this article were defrayed in part by the payment of page charges. This article must therefore be hereby marked "advertisement" in accordance with 18 U.S.C. Section 1734 solely to indicate this fact.

‡ To whom correspondence should be addressed. Tel.: 82-54-279-2128; Fax: 82-54-279-8159; E-mail: ihhwang@postech.ac.kr.

¹ The abbreviations used are: Tic, translocon of inner envelope membrane components; atToc159, *A. thaliana* Toc159; GFP, green fluorescent protein; WT, wild type.

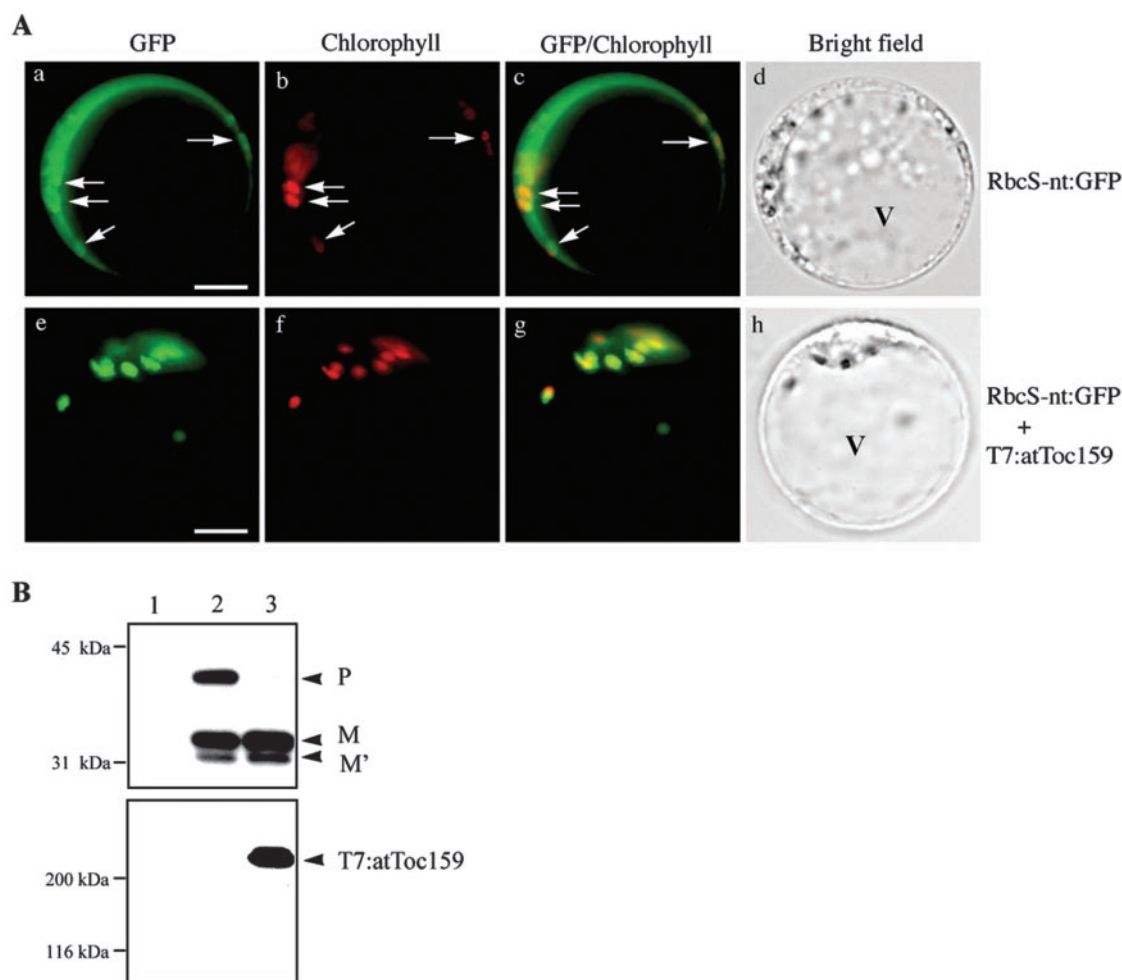


FIG. 2. Transiently expressed *atToc159* supports protein import into chloroplasts in protoplasts. *A*, localization of RbcS-nt:GFP. *ppi2* protoplasts were transformed with RbcS-nt:GFP alone or together with T7:atToc159, and localization of RbcS-nt:GFP was examined. Chlorophyll, autofluorescence of chlorophyll. Arrows indicate the punctate staining pattern of GFP signals overlapping the red autofluorescence of chlorophyll. V, vacuole. Bar = 20 μ m. *B*, Western blot analysis. Protein extracts were prepared from transformed protoplasts and used for Western blotting. RbcS-nt:GFP (top panel) and T7:atToc159 (bottom panel) were detected with anti-GFP and anti-T7 antibodies, respectively. Lane 1, protein extracts obtained from non-transformed *ppi2* protoplasts; lane 2, protein extracts obtained from *ppi2* protoplasts transformed with RbcS-nt:GFP alone; lane 3, protein extracts obtained from *ppi2* protoplasts transformed with RbcS-nt:GFP plus T7:atToc159. P, precursor form; M, mature form; M', a proteolytic product of the mature form.

sections (40–60 nm thick) were collected on uncoated nickel grids (300 mesh), stained with 4% uranyl acetate, and examined using a transmission electron microscope (Jeol 1200) at 60–80 kV.

Protein Fractionation and Gel Blot Analysis—Protein extracts were prepared as described previously (25). Whole-cell extracts were subjected to low-speed centrifugation (7000 \times *g*) at 4 $^{\circ}$ C for 5 min to eliminate cellular debris. The low-speed supernatant was further fractionated by ultracentrifugation at 100,000 \times *g* for 1 h. Whole-cell extracts or fractions were assayed by Western blotting using anti-GFP (Clontech, Inc) and anti-T7 (Novagen) antibodies. RbcS was detected with a polyclonal anti-Rbc antibody (26).

Transient Expression and in Vivo Targeting of Reporter Proteins—Plasmids were introduced by PEG-mediated transformation (25, 27) into *Arabidopsis* protoplasts prepared from leaf tissues. Expression of fusion constructs was monitored at various times after transformation, and images were captured with a cooled CCD camera and a Zeiss (Jena, Germany) Axioplan fluorescence microscope (25).

Immunohistochemistry—For immunohistochemistry, transformed protoplasts were prepared as described previously (28). Fixed cells were incubated with a mouse monoclonal anti-T7 antibody at 4 $^{\circ}$ C overnight and washed three times with TSW buffer. Subsequently, the cells were incubated with a fluorescein isothiocyanate-conjugated anti-mouse IgG (Zymed Laboratories Inc.) secondary antibody. Images were captured as described above.

RESULTS

Transient Expression of *atToc159* Supports Protein Import into Chloroplasts in *ppi2* Protoplasts—We investigated the role

of *atToc159* in protein import into chloroplasts using protoplasts derived from *Arabidopsis* leaf tissues as an experimental system. In this system, DNA constructs encoding reporter proteins destined for the chloroplasts were introduced into protoplasts by the polyethylene glycol-mediated transformation method (25, 27), and expression of the encoded proteins was monitored at various subsequent time points. We employed two different approaches to analyze the expression and targeting of the proteins. One is based on expressing fusion proteins including green or red fluorescent proteins (GFP or RFP), followed by image analysis using a fluorescent microscope. The other is based on Western blot analysis using antibodies to the expressed proteins. We employed a GFP fusion protein with the N-terminal transit peptide of the small subunit of rubisco complex (RbcS) as a reporter protein (Fig. 1A), as described previously (27). Fluorescence microscopy analyses revealed that RbcS-nt:GFP is efficiently imported into chloroplasts in protoplasts derived from leaf tissues of wild-type plants (Fig. 1B, panels d–f). In contrast, GFP alone was observed as a diffuse pattern in the cytosol (Fig. 1B, panels a–c). To further confirm the localization of RbcS-nt:GFP, we performed Western blotting using proteins obtained from RbcS-nt:GFP-transformed protoplasts. As shown in Fig. 1D, the majority of RbcS-nt:GFP was detected at 31 kDa (lane 3). Furthermore, the 31-kDa band

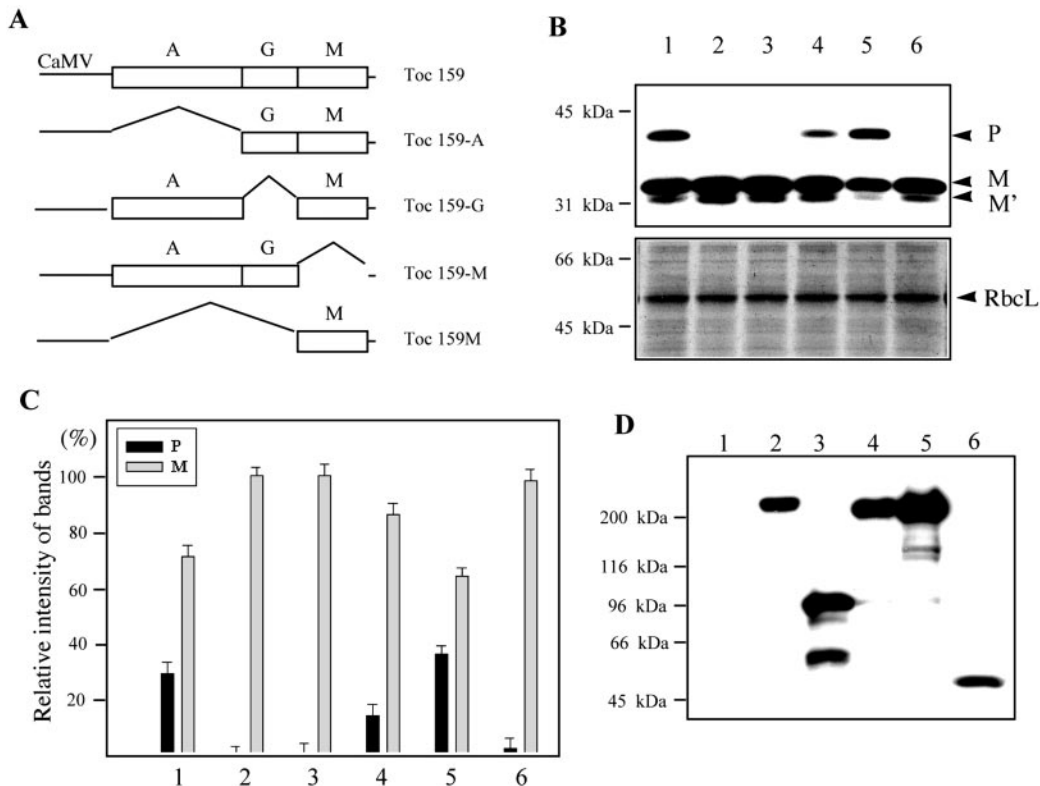


FIG. 3. The M domain is the minimal region required to support protein import into chloroplasts. *A*, schematics of various deletion mutants. *A*, *G*, and *M* indicate the N-terminal acidic domain, GTPase domain, and C-terminal membrane-anchored domain, respectively. CaMV, [³⁵S]CaMV promoter. All deletion mutants were tagged with T7 at the N terminus (not shown in the figure). *B*, Western blot analysis of protein import. *RbcS-nt:GFP* was transformed into protoplasts alone (*lane 1*), or together with atToc159 (*lane 2*), atToc159-A (*lane 3*), atToc159-G (*lane 4*), atToc159-M (*lane 5*), or atToc159M (*lane 6*). Protein extracts were prepared from transformed protoplasts 12 h after transformation and used to detect protein import by Western blotting with an anti-GFP antibody (*top panel*). An identical gel was stained with Coomassie Blue (*bottom panel*) to confirm equal loading of proteins. *P*, precursor form; *M*, mature form; *M'*, a proteolytic product. RbcL, the large subunit of the Rubisco complex. *C*, quantification of protein import. The intensity of each protein band in *B* was measured using image analysis software. The intensity was normalized to that of RbcL. The relative amounts of precursor and mature forms were calculated from the total amount (precursor plus mature) of RbcS-nt:GFP expressed in each condition. Identical experiments were performed three times to obtain the means and standard deviations. To maximize the difference in the signal intensity between bands, the exposure condition of Western blots was optimized by developing exposed films at two or three different time points. *Columns 1–6* are the same as those in *B*. *D*, expression of deletion mutants. Protein extracts were prepared from transformed protoplasts and used to detect expression of various deletion mutants by Western blotting with an anti-T7 antibody. Each lane is the same as in *B*.

co-purified with chloroplasts in a Percoll gradient (*lane 4*), indicating the presence of the protein within this organelle. A very weak band was sometimes detected at 39 kDa (the expected size of full-length RbcS-nt:GFP) in total protein extracts (*lane 3*) but not in chloroplast extracts (*lane 4*); this likely corresponds to the precursor RbcS-nt:GFP protein. The 31-kDa band may correspond to the mature protein because the N-terminal transit peptide of chloroplast proteins is proteolytically processed during import (1, 2). A band that is smaller than 31 kDa was also observed in the protein extracts, which may be a product of additional proteolytic processing in chloroplasts. Control GFP was detected at 29 kDa, as expected (Fig. 1D, *lane 2*).

Next we examined the import of RbcS-nt:GFP into chloroplasts in protoplasts derived from leaf tissues of *ppi2* plants. We examined whether proteins can be imported into the undeveloped chloroplasts in *ppi2* plants (8). *ppi2* protoplasts prepared from the white leaf tissues of *ppi2* plants were transformed with *RbcS-nt:GFP*, and the reporter protein was localized by observing its green fluorescence under a fluorescent microscope. As shown in Fig. 1C, a diffuse pattern of green fluorescent signals from RbcS-nt:GFP (*panels d–f*) was detected, and was similar to that of GFP alone (*panels a and c*) except for a few punctate stains (indicated by *arrows*). The narrow strip patterns of GFP signals observed in these protoplasts are due to the cytosol that is confined between the large

central vacuole and the plasma membrane. A similar result was obtained with other reporter proteins such as RA-nt:GFP (a GFP fusion protein with the transit peptide of rubisco activase) (data not shown). Interestingly, the GFP signals of RbcS-nt:GFP at the few punctate stains closely overlapped the red autofluorescence of chlorophyll, as depicted by the yellow signals (indicated by arrows, Fig. 1C, *panel f*). This suggests that although RbcS-nt:GFP is not efficiently imported into chloroplasts, some portion of RbcS-nt:GFP expressed in *ppi2* protoplasts may be imported into the undeveloped chloroplasts. To further confirm the GFP pattern of RbcS-nt:GFP in *ppi2* protoplasts, protein extracts were prepared from transformed *ppi2* protoplasts and examined by Western blot analysis using an anti-GFP antibody. RbcS-nt:GFP was detected as two strong bands at 31 and 39 kDa (Fig. 1D, *lane 5*). In *ppi2* protoplasts, the 39-kDa band was 40% ($\pm 5\%$, $n = 6$) of total expressed RbcS-nt:GFP and the 31-kDa band was 60% ($\pm 5\%$, $n = 6$), indicating that the amount of the precursor form is greatly increased in *ppi2* protoplasts compared with the wild-type protoplasts. These results are in agreement with the results obtained from the image analysis.

Next, we examined whether transient expression of atToc159 complements the loss of atToc159 with respect to protein import into chloroplasts in *ppi2* protoplasts. We generated atToc159 tagged with a small epitope (T7) at the N terminus for detection by Western blot. Protoplasts obtained from *ppi2*

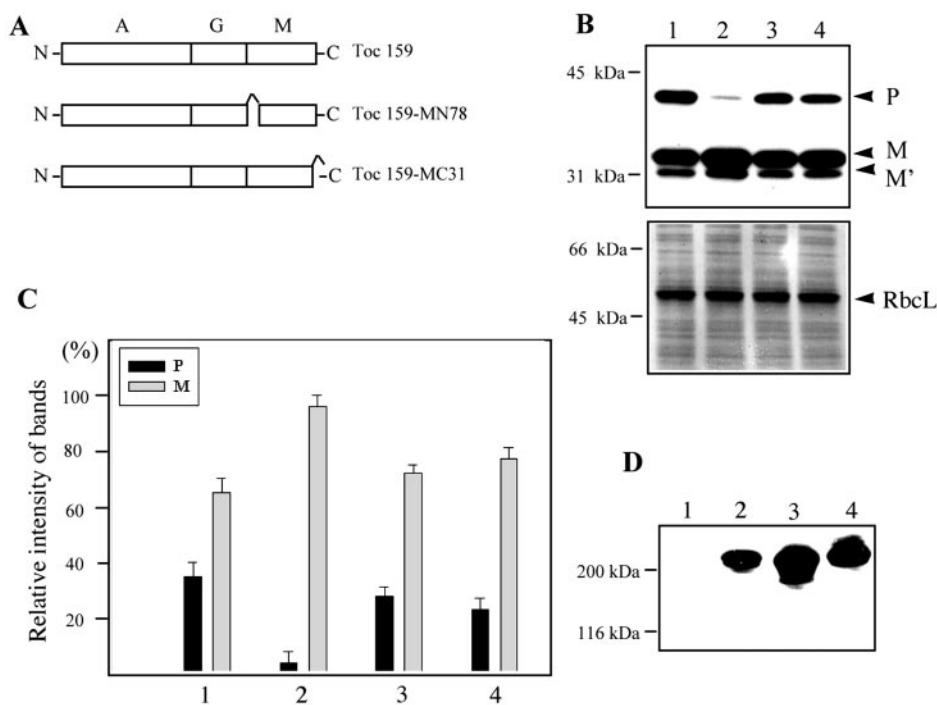


FIG. 4. An intact M domain is critical for protein import into chloroplasts. *A*, schematics of constructs. *B*, protein import assay. Protoplasts were transformed with RbcS-nt:GFP alone (lane 1) or together with *atToc159* (lane 2), *atToc159-MN78* (lane 3), or *atToc159-MC31* (lane 4). Protein extracts obtained from transformed protoplasts were analyzed as described for Fig. 3*B*. *C*, quantification of protein import was performed as described for Fig. 3*C*. Columns 1–4 are the same as those in *B*. *D*, expression of deletion mutants. Protein extracts were prepared from transformed protoplasts and employed to detect expression of deletion mutants by Western blotting with an anti-T7 antibody. Lanes 1–4 are the same as in *B*.

plants were co-transformed with two plasmids, *RbcS-nt:GFP* and *T7:atToc159*, and localization of the reporter protein was examined. When co-transformed with *T7:atToc159*, the green fluorescence of RbcS-nt:GFP was detected as punctate stains with no diffuse signals (Fig. 2*A*, panels *e* and *g*), in contrast to what was seen in *ppi2* protoplasts expressing RbcS-nt:GFP alone (panels *a* and *c*). Furthermore, these green punctate stains closely overlapped the red autofluorescence of chlorophyll. To further verify protein import in the presence of co-expressed *atToc159*, Western blotting was performed using proteins prepared from transformed *ppi2* protoplasts. As shown in Fig. 2*B* (top panel), RbcS-nt:GFP was detected mainly as the mature form, with nearly undetectable levels of precursor (lane 3), indicating that the protein is efficiently imported into chloroplasts. We additionally examined the expression of *atToc159* using an anti-T7 antibody. As shown in Fig. 2*B* (bottom panel), the monoclonal anti-T7 antibody specifically detected a band at 230 kDa (the expected position of *atToc159*) (lane 3) in protoplasts transformed with *RbcS-nt:GFP* together with *atToc159*, but not in those transformed with *RbcS-nt:GFP* alone (lane 2) or non-transformed protoplasts (lane 1).

The C-terminal M Domain Is Sufficient for Protein Import into Chloroplasts in *ppi2* Mutants—The next step was to identify the domain of *atToc159* that is critical for protein import into chloroplasts. Various deletion mutants were generated and tagged with T7 at the N terminus (Fig. 3*A*). Constructs were introduced into protoplasts along with *RbcS-nt:GFP*, and import of the fusion protein into chloroplasts was examined by Western blotting (Fig. 3, *B* and *C*). The degree to which these mutants complemented the defect in the protein import was assessed by measuring the reduction in the precursor form. In control protoplasts transformed with the vector alone, the precursor level was 35% of the total RbcS-nt:GFP (Fig. 3*B*, lane 1). In protoplasts expressing *atToc159-A* (lane 3) or *atToc159-M* (lane 6), the precursor form of RbcS-nt:GFP was nearly unde-

tectable, similar to that observed with full-length *atToc159* (lane 2). In the presence of *atToc159-G* (lane 4), the amount of precursor protein was 15% of the total RbcS-nt:GFP expressed, implying that the ability of this mutant to support protein import into chloroplasts was hampered but still functional. However, in protoplasts expressing *atToc159-M* (lane 5), the amount of precursor RbcS-nt:GFP was equivalent to that in protoplasts transformed with vector alone, indicating that the M domain is most critical for protein import into chloroplasts.

Expression of these mutant *atToc159* proteins in *ppi2* protoplasts was analyzed by Western blotting using the anti-T7 antibody. The deletion mutants were present at nearly equal levels in the protein extracts prepared from transformed protoplasts (Fig. 3*D*), confirming their expression in *ppi2* protoplasts. *atToc159-A* (lane 3) and *atToc159-M* (lane 6) were detected at the expected positions based on their calculated molecular weights, whereas the *atToc159* (lane 2), *atToc159-G* (lane 4), and *atToc159-M* (lane 5) bands were much larger than their expected sizes. *Toc159* has previously been detected at 230 kDa instead of 159 kDa (the calculated molecular weight of *Toc159*) (29). The migration patterns of these deletion mutants strongly suggest that the abnormal mobility of *atToc159* is due to the A domain.

To further define the domain necessary for protein import into chloroplasts, we generated additional mutants, *atToc159-MN78* and *atToc159-MC31* (Fig. 4*A*). The *atToc159-MN78* mutant underwent a 78-amino acid deletion from the N-terminal side of the M domain, while *atToc159-MC31* has a 31-amino acid deletion from the C terminus of the M domain. The deletion mutants were introduced into *ppi2* protoplasts together with *RbcS-nt:GFP*. Protein extracts were prepared and RbcS-nt:GFP import was examined by Western blot. As depicted in Fig. 4, *B* and *C*, ~29% of RbcS-nt:GFP was detected as the precursor form upon co-expression with *atToc159-MN78* (lane 3), and 24% was detected as precursor when RbcS-nt:GFP was

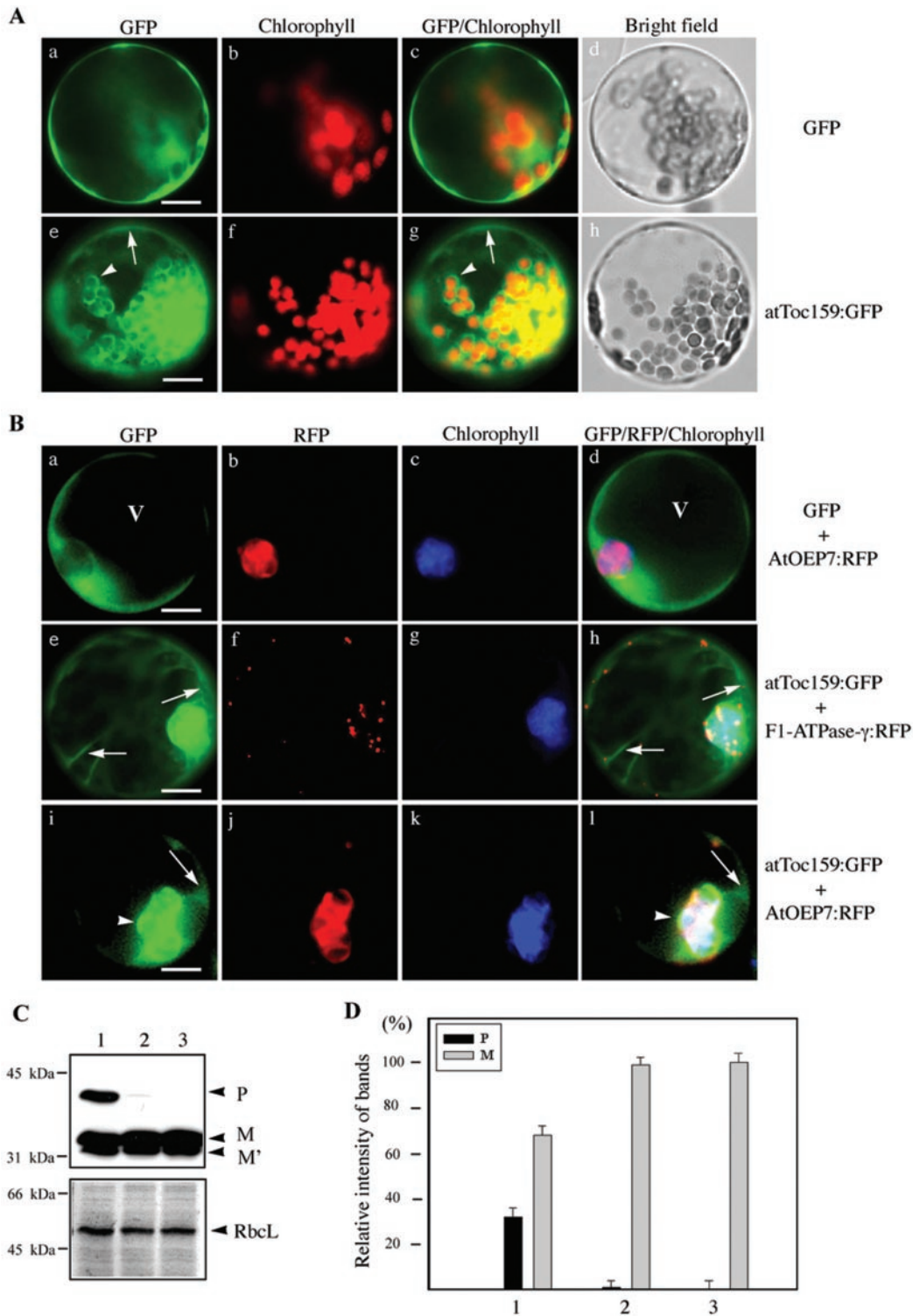


FIG. 5. A GFP-tagged form of *atToc159* localizes to both the cytosol and chloroplasts in wild-type and *ppi2* protoplasts. A, localization of *atToc159*:GFP in wild-type protoplasts. Protoplasts obtained from wild-type plants were transformed with *GFP* on its own or *atToc159*:GFP and localization of these proteins was examined. *Arrows* and *arrowheads* indicate GFP signals at the cytosol and chloroplast envelope membrane, respectively. *Bar* = 20 μ m. **B**, localization of *atToc159*:GFP in *ppi2* protoplasts. *ppi2* protoplasts were transformed with *GFP* plus *AtOEP7*:RFP, *atToc159*:GFP plus *F1-ATPase-γ*:RFP, or *atToc159*:GFP plus *AtOEP7*:RFP, and localization of these proteins was examined 24 h after transformation. *RFP*, red fluorescent protein; *Chlorophyll*, autofluorescence of chlorophyll (depicted in *blue*). *Arrows* and *arrowheads* indicate GFP signals at the cytosol and chloroplast envelope membrane, respectively. *V*, vacuole. *Bar* = 20 μ m. **C**, protein import assay. *ppi2* protoplasts were transformed with *RbcS-nt*:GFP alone (*lane 1*) or together with *atToc159* (*lane 2*) or *atToc159*:GFP (*lane 3*). Protein extracts were analyzed as described for Fig. 3(B). *P*, precursor form; *M*, mature form; *M'*, a proteolytic product. *RbcL*, the large subunit of the Rubisco complex. **D**, quantification of protein import was performed as described for Fig. 3C. *Columns 1–3* are the same as in **C**.

co-expressed with *atToc159*-MC31 (*lane 4*). In the control protoplasts transformed with *RbcS-nt*:GFP alone, 35% of the *RbcS-nt*:GFP was in the precursor form. Expression of the

atToc159-MN78 and *atToc159*-MC31 mutant proteins was confirmed by Western blotting using the anti-T7 antibody (Fig. 4D). Our results strongly suggest that the intact M domain is

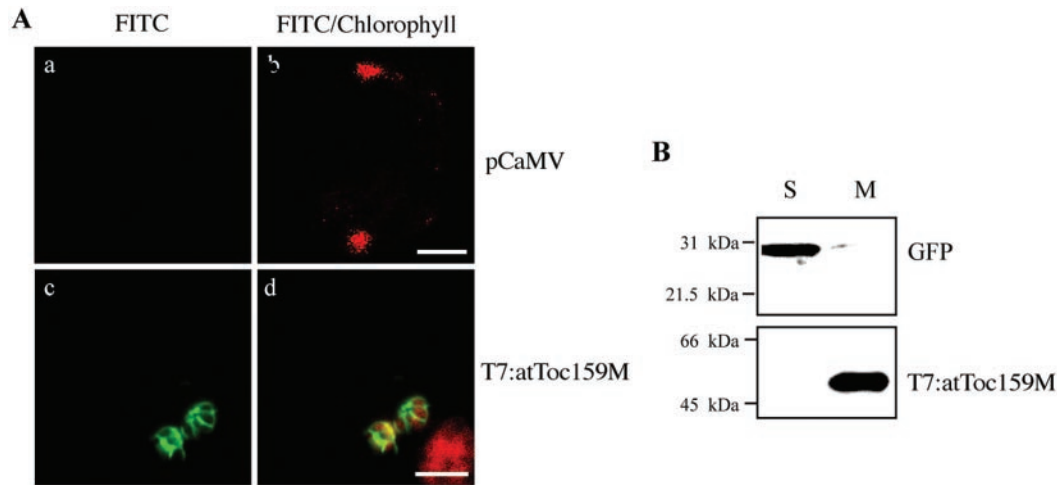


FIG. 6. *atToc159M* is targeted to the chloroplast. *A*, localization of *atToc159M*. *ppi2* protoplasts were transformed with *pCaMV* (a control plasmid with only the promoter) or *T7:atToc159M*, and localization was examined by immunohistochemistry using an anti-T7 antibody. *CH*, autofluorescence of chlorophyll. *Bar* = 20 μ m. *B*, subcellular fractionation of *atToc159M*. Protein extracts were obtained from protoplasts transformed with *T7:atToc159M* and *GFP*, and fractionated into soluble (*S*) and membrane (*M*) fractions by ultracentrifugation. The presence of *GFP* and *T7:atToc159M* was detected by Western blot analysis with anti-*GFP* and anti-T7 antibodies, respectively.

necessary to support protein import into chloroplasts.

The M Domain Alone Is Targeted to Chloroplasts—Earlier studies have shown that *Toc159* is present in both membrane-associated and soluble forms (29), and that the G domain plays a critical role in the targeting of the protein to the outer envelope membrane (21, 22). However, the fact that the M domain is sufficient to support protein import into chloroplasts in *ppi2* protoplasts raises the possibility that the isolated M domain may also be targeted to chloroplasts. Thus, we examined the localization of *atToc159* and the M domain. We generated GFP-tagged *atToc159* by inserting the GFP coding region between the A and G domains; the resulting construct was introduced into protoplasts of wild-type plants. As shown in Fig. 5A (panels e–g), *atToc159:GFP* localized to chloroplasts with a ring pattern, an indication of localization in the envelope membrane. In addition, the GFP signal was detected in the cytosol (the area where the red autofluorescent signals of chlorophyll are not detected) as a diffuse pattern, signifying that a part of *atToc159:GFP* is also present in the cytosol, consistent with previous data (21, 22). GFP alone gave a diffuse pattern (Fig. 5A, panels a–c).

Next we examined the targeting of *atToc159:GFP* to chloroplasts in *ppi2* protoplasts. Protoplasts were transformed with *atToc159:GFP* together with *AtOEP7:RFP*, a fusion protein of the outer envelope membrane protein *AtOEP7* and RFP that is targeted to the outer envelope membrane of chloroplasts (30). As shown in Fig. 5B (panels i and l), *atToc159:GFP* again displayed a diffuse pattern together with a ring pattern. The ring pattern of the *atToc159:GFP* signal closely overlapped that of the *AtOEP7:RFP* signal (panels i, j, and l). Furthermore, GFP and RFP signals surrounded the autofluorescence signals of chlorophyll (panels i–l). These results collectively suggest that *atToc159:GFP* localizes to both the cytosol and to the undeveloped chloroplasts in *ppi2* protoplasts. As a control, we transformed *ppi2* protoplasts with GFP and *AtOEP7:RFP* and examined the localization of these proteins. GFP on its own gave a diffuse pattern and did not overlap the red fluorescent signals of *AtOEP7:RFP* (Fig. 5B, panels a–d). However, as expected, the red fluorescent signals of *AtOEP7:RFP* surrounded the autofluorescent signals of chlorophyll. As another control for the localization of *atToc159* to the chloroplast envelope membrane, we transformed *ppi2* protoplasts with *atToc159:GFP* with *F1-ATPase- γ :RFP*, a mitochondrial marker generated by fusion of the transit peptide of mitochondrial

F1-ATPase- γ with RFP (31). As expected, the red signals of *F1-ATPase- γ :RFP* gave a punctate staining pattern that did not overlap green signals of *atToc159:GFP* (Fig. 5B, panels e–h), although the red punctate stains of the mitochondria were concentrated around the chloroplasts, as often occurs in plant cells. To determine whether the GFP domain affects *atToc159* activity, we performed a complementation assay in *ppi2* protoplasts using *atToc159:GFP*. *atToc159:GFP* supported the import of *RbcS-nt:GFP* as efficiently as *atToc159* (Fig. 5, C and D, lanes 2 and 3), confirming that the GFP domain insertion into *atToc159* does not affect the function of the protein.

We then investigated the localization of the M domain using a form with a GFP tag at the N terminus. The *atToc159M:GFP* fusion protein was not targeted to chloroplasts, but formed large aggregates for reasons that are unknown at present (data not shown). We also examined the localization of the T7-tagged M domain, *T7:atToc159M*, by immunohistochemical analysis using the T7 antibody. The green fluorescence of *atToc159M* was observed as a ring pattern surrounding the red autofluorescence of chlorophyll in *ppi2* protoplasts (Fig. 6A, panels c and d), suggesting that *atToc159M* is targeted to the envelope membranes of chloroplasts. In control protoplasts transformed with vector alone (Fig. 6A, panels a and b), no green signal was observed, confirming the specificity of the anti-T7 antibody. To further establish the localization of *atToc159M*, protein extracts prepared from *ppi2* protoplasts co-transformed with *T7:atToc159M* and *GFP* were fractionated into membrane and soluble fractions. Co-expressed GFP was used as a control for soluble proteins in the subcellular fractionation. As shown in Fig. 6B, *T7:atToc159M* was detected in the membrane fraction, but not the soluble fraction, whereas GFP alone was present in the soluble fraction.

The GTPase Domain Is Critical for Protein Import into Chloroplasts—We next assessed the role of the GTPase domain (G domain) in protein import into chloroplasts. The G domain plays an essential role in the targeting of *Toc159* to the outer membrane of chloroplasts (21, 22). Mutations were introduced in the first and second GTP-binding motifs to generate *atToc159[S/N]* and *atToc159[D/L]*, respectively, and were tagged with T7 at the N terminus (Fig. 7A). The substitution of serine (S) with asparagine (N), *atToc159[S/N]*, at the first GTP binding motif of GTP-binding proteins produces a GDP-bound form, whereas the substitution of aspartic acid (D) with leucine (L), *atToc159[D/L]*, at the second GTP-binding motif generates

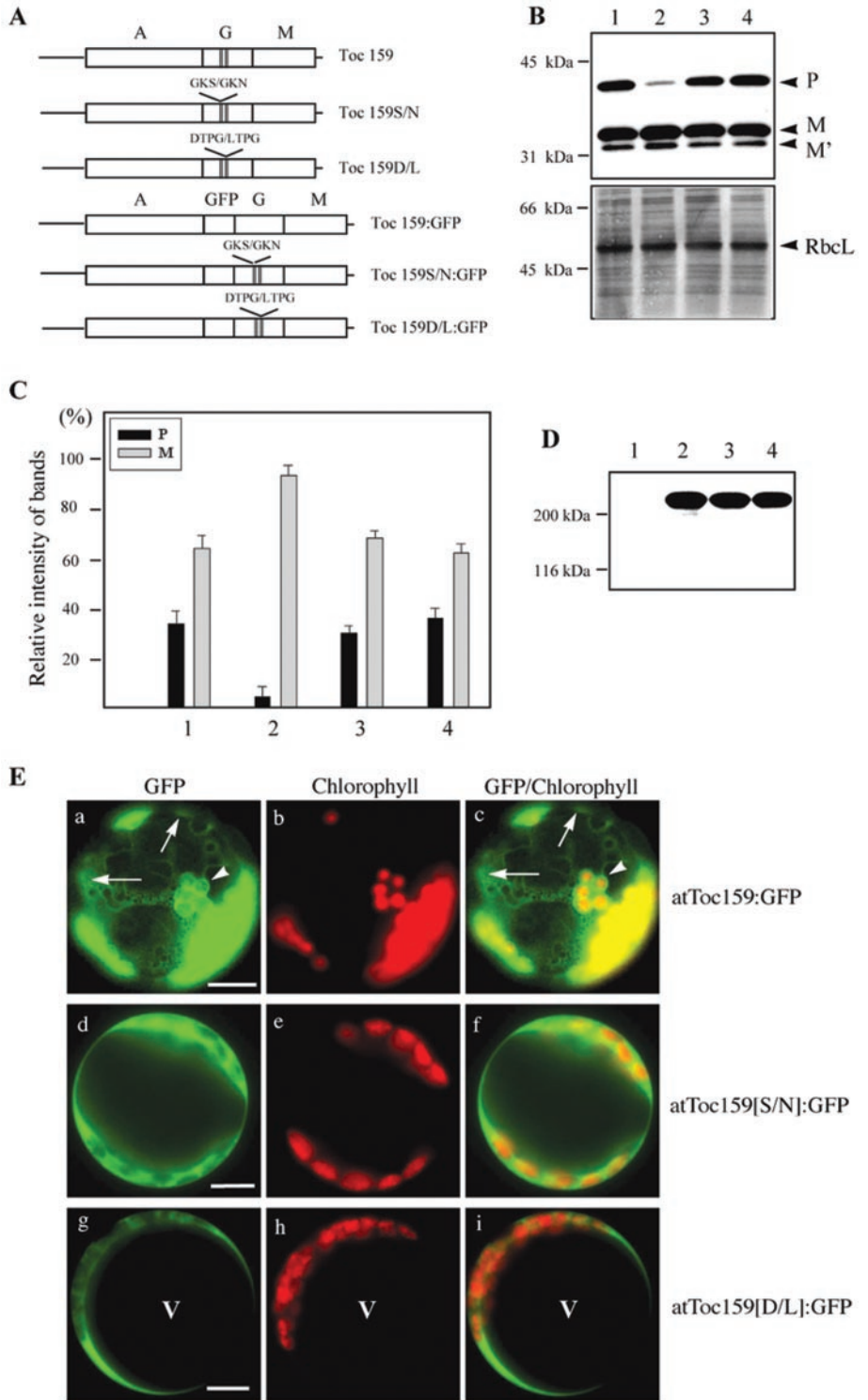


FIG. 7. The G domain is critical for protein import into chloroplasts. *A*, schematics of constructs. Mutations in the first and second GTP-binding motifs are indicated. The serine (amino acid position 869) in the first GTP-binding motif was replaced with asparagine (S/N) and the glutamic acid (amino acid position 909) at the second GTP-binding motif was changed to leucine (D/L). The GFP domain was inserted between the A and G domains. *B*, protein import assay. Protoplasts were transformed with *RbcS-nt::GFP* alone (lane 1) or together with *atToc159* (lane 2), *atToc159[S/N]* (lane 3), or *atToc159[D/L]* (lane 4). Protein extracts obtained from protoplasts were analyzed as described for Fig. 3*B*. *C*, quantification of protein import was performed as described for Fig. 3*C*. Columns 1–4 are the same as in *B*. *D*, expression of substitution mutants. Protein extracts were prepared from transformed protoplasts and used to detect expression of substitution mutants by Western blotting with an anti-T7 antibody. Lanes 1–4 are the same as in *B*. *E*, localization of proteins. Protoplasts were transformed with the indicated constructs. Localization of these proteins was examined 24 h after transformation. Arrows and arrowheads indicate GFP signals in the cytosol and chloroplast envelope membrane, respectively. V, vacuole. Bar = 20 μ m.

a GTPase-defective mutant form (32). The mutants, *T7:Toc159[S/N]* and *T7:Toc159[D/L]*, were introduced into *ppi2* protoplasts along with *RbcS-nt::GFP*, and targeting of *RbcS-nt::GFP* was examined. In the presence of both *atToc159[S/N]* and *atToc159[D/L]*, 30 to 35% of *RbcS-nt::GFP* was detected as the precursor form (Fig. 7, *B* and *C*), similar to that in control protoplasts. This result is in accordance to previous studies that showed that the G domain is critical for targeting of *Toc159* to chloroplasts (21, 22). However, this result appeared to be in contrast to the above results showing that the M domain is targeted to the chloroplasts and is sufficient to complement the defect of protein import into chloroplasts in *ppi2*

protoplasts. One possible explanation is that the mutant G domains may have a dominant negative effect on *atToc159* with respect to its targeting to chloroplasts. To confirm that these proteins are expressed in protoplasts, protein extracts were prepared from protoplasts transformed with these mutants and analyzed by Western blotting using the anti-T7 antibody. Similar levels of *atToc159[S/N]* (lane 3), *atToc159[D/L]* (lane 4), and wild-type *atToc159* (lane 2) were observed in protoplasts (Fig. 7*D*).

To further investigate the failure of *atToc159[S/N]* and *atToc159[D/L]* to support protein import into chloroplasts in *ppi2* protoplasts, we examined the localization of these mu-

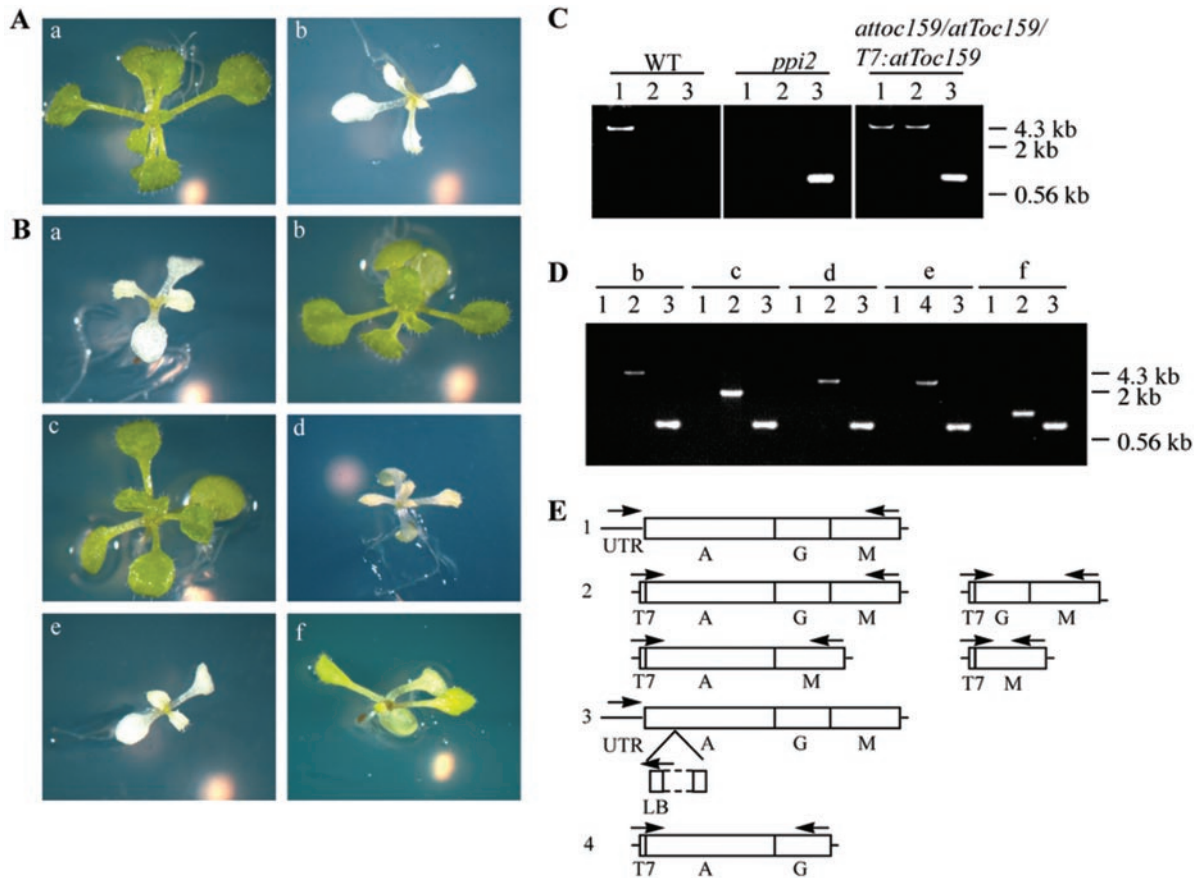


FIG. 8. The M domain complements *ppi2* mutants in transgenic plants. **A**, phenotype of wild-type (*a*) and *ppi2* (*b*) plants. **B**, phenotype of transgenic plants. Transgenic plants were generated with various deletion constructs as specified below. Transgenic plants expressing the indicated proteins in the *ppi2* homozygote background were selected from the T2 generation. Plants were grown on MS plates for 10 days. *a*, pBI122; *b*, *atToc159*; *c*, *atToc159-A*; *d*, *atToc159-G*; *e*, *atToc159-M*; *f*, *atToc159M*. All plants displayed a *ppi2* background, as confirmed below in **C** and **D**, genotype analysis of transgenic plants. Genomic DNA samples were obtained from rosette leaves of individual plants and used for PCR amplification as depicted in **E**. *ppi2*, *ppi2* homozygote; *attoc159/atToc159/T7:atToc159*, heterozygotes harboring the transgene *T7:atToc159*. Panels *b-f* are the same in **B**. The numbers 1–4 are depicted in **E**. **E**, location of PCR primers for PCR. A, G, and M are the A, G, and M domains, respectively. UTR, 5'-untranslated region of *atToc159*; LB, left border; T7, T7 tag. The numbers 1–4 indicate the lanes in **D**.

TABLE I
Phenotype analysis of the T2 generation of transgenic plants

T2 generation of plants were grown on plates containing both kanamycin (50 mg/liter) and hygromycin (45 mg/liter). The plants scored in the table are resistant to both kanamycin and hygromycin. The phenotype was scored 10 days after germination. Note that plants sensitive to kanamycin and/or hygromycin died and are not included in the table.

Constructs introduced	Phenotype of plants			
	Green	Greenish	Yellowish	Albino
Vector (pBI122)	93			49
T7: <i>atToc159</i>	134			2
T7: <i>atToc159-A</i>	128			3
T7: <i>atToc159-G</i>	85		47	
T7: <i>atToc159-M</i>	112			57
T7: <i>atToc159M</i>	133	62	7	0

tants. Again, the GFP coding region was inserted between the A and G domains and the resulting constructs were introduced into wild-type protoplasts. Both *atToc159*[S/N]:GFP (panels *d-f*) and *atToc159*[D/L]:GFP (panels *g-i*) were observed only as diffuse patterns in the cytosol (Fig. 7E). Our data indicate that the G domain is critical for targeting to the outer envelope membrane as observed previously (21, 22). Thus it is possible that the mutant G domain may mask the targeting signal present at the M domain, which in turn results in failure to support protein import into chloroplasts.

Chloroplasts Are Well Developed in Transgenic Plants Expressing the M Domain in *ppi2* Mutant Backgrounds—To con-

firm the results obtained with the transient expression approach in *ppi2* protoplasts, we generated transgenic plants expressing various deletion mutants in a *ppi2* background. The *ppi2* mutant was maintained as heterozygotes, since homozygotes are seedling lethal (Fig. 8A, panel *b*) (8). Transformation was performed using heterozygote plants at the *atToc159* locus. Heterozygotes were similar to wild types in appearance and were selected from a pool of seeds obtained from heterozygous plants based on wild-type appearance and kanamycin resistance. Transformants were selected using both kanamycin and hygromycin resistance, since deletion mutants were introduced into plants together with the hygromycin-resistance gene. We scored the phenotype and segregation of transgenic plants at the T2 generation on plates containing both kanamycin and hygromycin. A summary of the segregation ratios from transgenic plants is shown in Table I. As expected from transgenic plants transformed with the vector (pBI-Hyg), all the plants resistant to both kanamycin and hygromycin were nearly identical to *ppi2* homozygotes (Fig. 8B, panel *a*). When *atToc159* and *atToc159-A* were introduced into *ppi2* heterozygotes, most of plants resistant to both kanamycin and hygromycin were wild-type plants (Fig. 8B, panels *b* and *c*), indicating that these proteins complement the mutation. Moreover, *atToc159-A* transgenic plants (Fig. 8B, panel *c*) were nearly identical to wild-type plants (Fig. 8A, panel *a*), suggesting that the A domain is dispensable. Upon introduction of *atToc159-G*, we observed yellowish (Fig. 8B, panel *d*) and wild-type plants (data

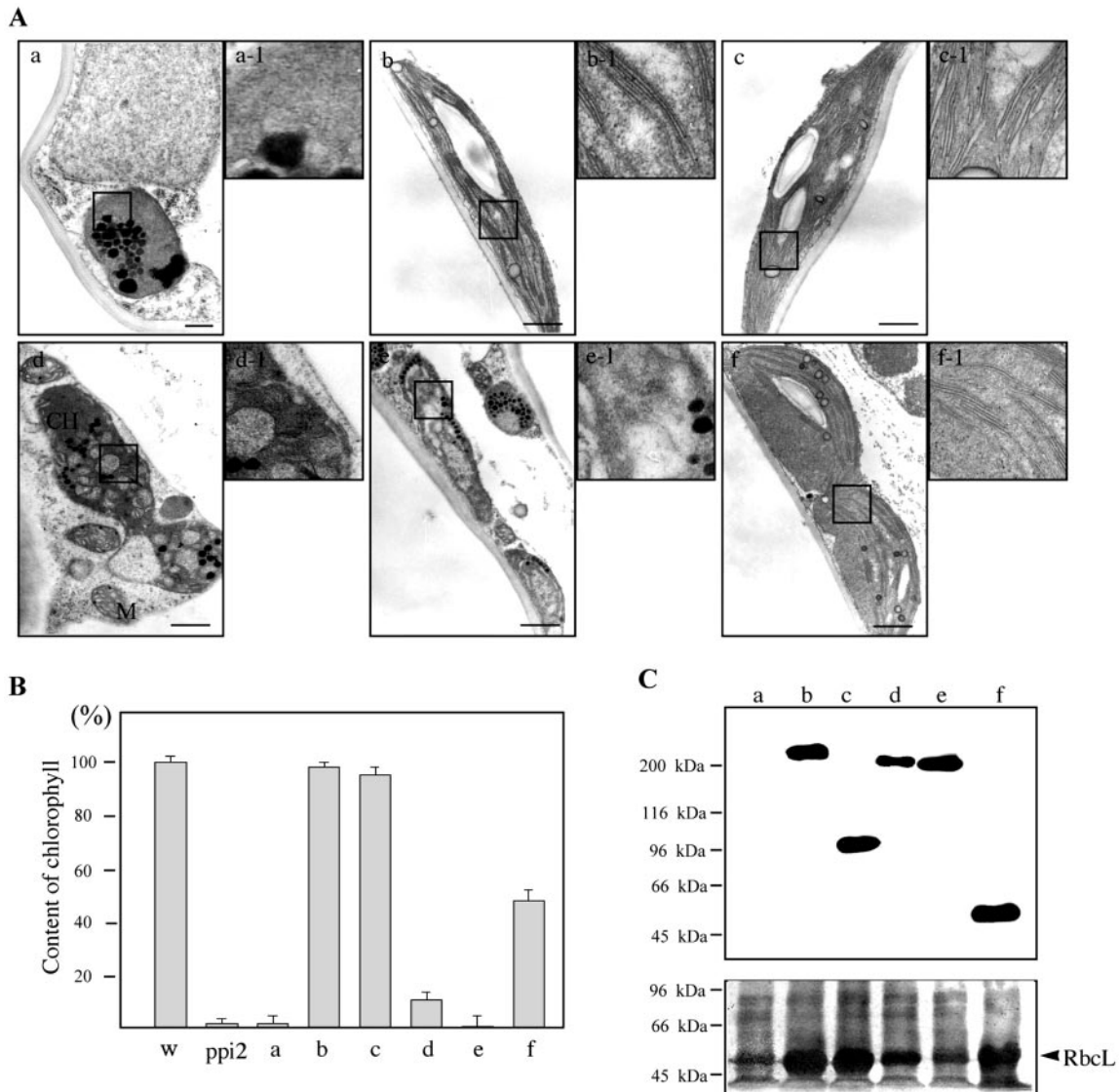


FIG. 9. Ultrastructural analysis of transgenic plants. *A*, chloroplast morphology at the EM level. Ultra-thin sections were prepared and examined with a transmission electron microscope. Enlarged images are from the boxed areas. *a*, pBI122; *b*, atToc159; *c*, atToc159-A; *d*, atToc159-G; *e*, atToc159-M; *f*, atToc159M. All these plants have a *ppi2* background, as confirmed in Fig. 8B. Bar = 200 nm. *B*, chlorophyll content. The amount of chlorophyll was measured in triplicate to obtain means and standard deviations. *ppi2*, *ppi2* homozygote. Columns *a-f* are the same as in *A*. *C*, expression of deletion mutants in transgenic plants. Protein extracts were prepared from transgenic plants and used for Western blot analysis with an anti-T7 antibody. Lanes *a-f* are the same as in *A*. RbcL, the large subunit of the rubisco complex.

not shown), but no albino plants among plants that were resistant to both kanamycin and hygromycin. The ratio of yellowish to wild-type plants was nearly 1 to 2, suggesting that the yellow plants represent homozygous *ppi2* plants expressing atToc159-G, which weakly complements the loss of atToc159. When we examined transgenic plants obtained with *atToc159-M*, albino (Fig. 8B, panel *e*) and wild-type plants (data not shown) were observed, as is the case in plants obtained with the vector alone. Furthermore, the segregation ratio of T2 progeny was 1 to 2 (albino to wild-type plants), indicating that atToc159-M does not complement the loss of atToc159 in *ppi2*. Among atToc159M transgenic plants that were resistant to both kanamycin and hygromycin, greenish (Fig. 8B, panel *f*) or wild-type plants (but no albino plants) were observed. The ratio of greenish to wild-type plants was 1 to 2, indicating that greenish plants are *ppi2* homozygotes with atToc159M. This finding strongly suggests that atToc159M functionally complements the loss of atToc159 at a slightly reduced efficiency compared with wild-type atToc159.

To further confirm the complementation, we examined the

genotypes of individual plants (Fig. 8A) by polymerase chain reaction with specific primers (Fig. 8E). As a control, PCR products obtained from homozygotes, heterozygotes harboring a copy of *atToc159*, and wild-type plants were compared. As expected, *ppi2* homozygote plants displayed no *atToc159* band with 5'- and 3'-primers but produced a T-DNA-specific band (800 bp) with LB and 5'-specific primers (lane 3) (Fig. 8B, panel *ppi2*). Heterozygotes harboring T7:atToc159 (*attoc159/atToc159/T7:atToc159*) exhibited atToc159 (lane 1), T7:atToc159 (lane 2), and T-DNA-specific (lane 3) bands at 4.6 kb, 4.5 kb, and 800 bp, respectively. In contrast, wild-type plants (WT) displayed only the *atToc159* band (lane 1, 4.6 kb), but no T-DNA band, as expected. Next, we examined the genotypes of transgenic plants harboring the various forms of *atToc159*. We selected plants resistant to both hygromycin and kanamycin from transgenic lines harboring the various deletion constructs (Fig. 8B). As shown in Fig. 8C, plants with a wild-type appearance transformed with *atToc159* (panel *b*) or *atToc159-A* (panel *c*) displayed both T-DNA-specific (800 bp) and transgene-specific bands, but not the endogenous *atToc159* band (Fig. 8D).

Kanamycin and hygromycin-resistant albino plants obtained from transgenic plants transformed with *atToc159-M* also exhibited T-DNA and transgene-specific bands, but not the endogenous *atToc159* band (panel e). Finally, yellowish (panel d) and greenish (panel f) plants also contained T-DNA-specific and transgene-specific bands but not the endogenous *atToc159* band, confirming that these phenotypes are a result of expression of *atToc159-G* and *atToc159M*, respectively, in a homozygous *ppi2* background. Thus, the various deletion mutants have different abilities to complement the loss of *atToc159* in *ppi2* plants; specifically, *atToc159* and *atToc159-A* have the capacity for full complementation, *atToc159-M* does not complement the loss of *atToc159*, *atToc159-G* provides only very weak complementation, and *atToc159M* has the capacity for nearly full complementation.

We examined the structures of ultra-thin sections of leaf tissues using transmission electron microscopy. We observed that albino plants obtained from transgenic lines harboring the vector alone had undeveloped chloroplasts with numerous lipid bodies but no thylakoid membranes (Fig. 9A, panel a), in accordance with previous data (8). However, as expected from the phenotype, chloroplasts in transgenic plants harboring *atToc159* (panel b) and *atToc159-A* (panel c) were fully developed, with numerous stacks of thylakoid membranes. In contrast, chloroplasts in transgenic plants harboring *atToc159-G* were not fully developed and contained only a few strands of thylakoid membranes (panel d). In transgenic plants harboring *atToc159-M*, chloroplast morphology was similar to that observed in *ppi2* plants (panel e). In transgenic plants with *atToc159M*, chloroplasts were well developed, as judged by density of thylakoid membranes (panel f), which were similar to those in transgenic plants with *atToc159* or *atToc159-A*. However, careful analyses revealed that the density of thylakoid membranes was slightly lower in transgenic plants with *atToc159M* than in those with *atToc159*. These results confirm the phenotypic results in whole plants.

To obtain independent evidence of the degree of complementation by the deletion mutants of *atToc159*, we measured the chlorophyll content as a marker for complementation. *ppi2* plants expressing *atToc159* or *atToc159-A* displayed nearly identical chlorophyll content (Fig. 9B). Transgenic plants with *atToc159-M* were nearly identical to *ppi2* with regard to chlorophyll content. Transgenic plants with *atToc159-G* and *atToc159M* displayed 10 and 50% of the chlorophyll content observed in wild-type plants, respectively. These results are in agreement with the data obtained from the experiments described above.

Next, we performed Western blotting with protein extracts obtained from transgenic plants using an anti-T7 antibody to confirm the expression of the various forms of *atToc159* in transgenic plants. Similar levels of protein were expressed by the deletion mutants and wild-type *atToc159* (Fig. 9C).

Finally, we examined the localization of *atToc159M* with immunohistochemistry using a monoclonal anti-T7 antibody, with a view to elucidating the mechanism of complementation by the *atToc159M* mutant. As depicted in Fig. 10A (panels d and e), *atToc159M* was detected as a ring pattern around chloroplasts, indicating that it is targeted to chloroplasts. In contrast, no signal was detected from wild-type plants, confirming the specificity of the anti-T7 antibody. To confirm the presence of *atToc159M* at the envelope membrane, protein extracts obtained from transgenic plants with *atToc159M* were fractionated into membrane and soluble fractions by ultracentrifugation. The presence of *atToc159M* in these fractions was determined by Western blot analysis with the anti-T7 antibody. *atToc159M* was detected in the membrane, but not the soluble

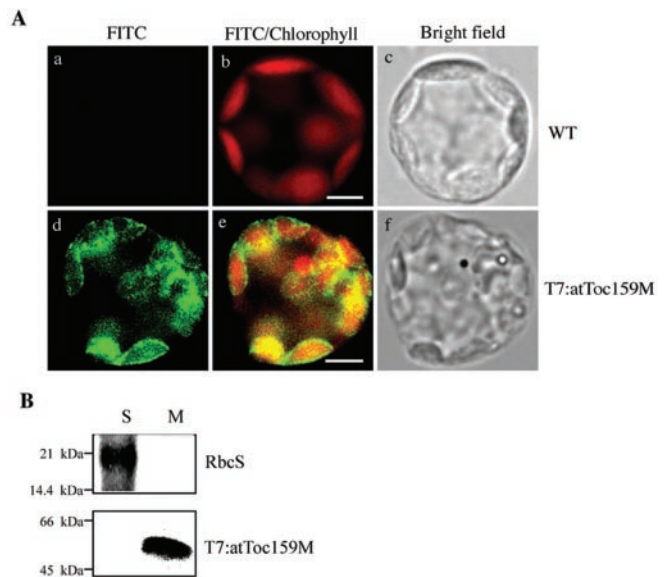


FIG. 10. *atToc159M* is targeted to the chloroplast envelope membrane in transgenic plants. A, localization of T7:*atToc159M*. Leaf protoplasts obtained from transgenic lines expressing T7:*atToc159* (T7:*atToc159M*) or non-transgenic plants (WT) were fixed and stained with an anti-T7 antibody. Ch, autofluorescence of chlorophyll. Bar = 20 μ m. B, membrane association of *atToc159M*. Protein extracts prepared from leaf tissues of transgenic plants expressing *atToc159M* in a *ppi2* background were fractionated into soluble (S) and membrane (M) fractions by ultracentrifugation. The presence of T7:*atToc159M* in these fractions was detected by Western blot analysis using an anti-T7 antibody. As a control for soluble proteins, RbcS was detected with a polyclonal anti-Rbc antibody.

fraction (Fig. 10B, top panel). As a control, we also used an anti-Rbc antibody and found that RbcS is specifically detected in the soluble fraction (Fig. 10B, bottom panel).

DISCUSSION

In this study we established that the loss of protein import into chloroplasts due to the absence of *atToc159* in *ppi2* mutants can be complemented by transiently expressing *atToc159* in protoplasts. This transient expression system in protoplasts has been shown to be a convenient way to study protein import into chloroplasts (27), despite certain potential limitations, such as possible mislocalization of proteins due to overexpression and alterations in responses due to the absence of the cell wall (33). In *ppi2* protoplasts, RbcS-nt:GFP was partially imported into chloroplasts, as expected due to the loss of *atToc159*. The import of RbcS-nt:GFP in *ppi2* protoplasts despite the loss of *atToc159* may be due to the presence of other *atToc159* homologs, such as *atToc132*, *atToc120*, and *atToc90* (8, 34). However, the amount of imported RbcS-nt:GFP was 60% of the total amount of RbcS-nt:GFP expressed in protoplasts. This seems to contradict a previous study, which showed only a small amount of RbcS is present in *ppi2* plants (8). This may be due to a difference in expression between endogenous RbcS and our RbcS-nt:GFP construct, which is under the control of the strong CaMV promoter. By this logic, the small amount of RbcS accumulated in *ppi2* mutants may not directly reflect the protein import capacity *per se* in *ppi2* plants. Rather, the defect in protein import into chloroplasts may also cause a defect in the expression of RbcS in *ppi2* plants, possibly due to a lack of a positive feedback signaling from the chloroplast to the nucleus (35). In contrast, expression of RbcS-nt:GFP derived from the strong CaMV ³⁵S-promoter in *ppi2* protoplasts is not likely to be affected by the lack of chloroplast development.

From our experiments using transient and transgenic ex-

pression of various deletion mutants of atToc159 in *ppi2* protoplasts, we conclude that the M domain alone fully complements the loss of atToc159 with respect to protein import into chloroplasts. In transgenic plants expressing atToc159M in a *ppi2* background, atToc159M nearly fully complemented the loss of atToc159 with respect to the density of the thylakoid membrane. However, measurement of the degree of complementation by chlorophyll content revealed that transgenic plants with atToc159M in a *ppi2* background displayed 50% of the chlorophyll content of wild types, suggesting that the M domain complements the loss of atToc159 with reduced efficiency compared with the full-length protein.

Previous findings suggest that the G domain is essential for the targeting of Toc159 (21, 22). We also confirmed the importance of the G domain for atToc159 targeting as well as the ability of the protein to support protein import into chloroplasts. When atToc159[S/N] and atToc159[D/L] were expressed transiently in *ppi2* protoplasts, mutant proteins were observed in the cytosol and did not support protein import into chloroplasts. The A domain, in contrast, is dispensable for complementation with respect to protein import into chloroplasts in protoplasts as well as in transgenic plants with the *ppi2* background. Interestingly, in both *ppi2* protoplasts and transgenic plants, the isolated M domain was targeted to the chloroplast envelope membrane and co-fractionated with the membrane. This result appears to be inconsistent with previous studies (21, 22) and with the data obtained with atToc159[S/N] and atToc159[D/L] in this study. One possible explanation for this discrepancy is that the M domain itself contains the information to target Toc159 to chloroplasts, but targeting of atToc159 to the chloroplast envelope membrane is regulated by the G domain. A possible mechanism for this process is that the targeting signal, a part of the M domain, is masked by the G domain when it is present in the cytosol. Targeting of atToc159 to the chloroplast outer envelope membrane would occur when the targeting signal at the M domain is exposed after conformational changes of the G domain upon GTP hydrolysis. As proposed previously, the G domain of atToc159 may interact with atToc34 to activate the GTPase activity of atToc159 for targeting and/or insertion into the envelope membrane (21, 22). Thus, deletion of both the A and G domains may result in the exposure of targeting signal, allowing the isolated M domain to be targeted to the chloroplast envelope membrane; point mutations in the G domain, such as we introduced, would not expose the targeting signal. Although the isolated M domain may be targeted to the membrane at a lower efficiency, it is nevertheless sufficient to support protein import into chloroplasts in *ppi2* protoplasts.

The transient expression of atToc159M is necessary and sufficient for protein import into chloroplasts in *ppi2* protoplasts. However, in transgenic plants expressing atToc159M in the *ppi2* background, the chlorophyll content was ~50% that of the wild type, indicating that it does not fully complement the loss of atToc159 in *ppi2* mutants. The importance of atToc159 in chloroplast biogenesis is clearly demonstrated, as shown by the *ppi2* phenotype (8). However, its mechanism of action *in vivo* remains to be elucidated, despite numerous reports that Toc159 at the envelope membrane is involved in protein import into chloroplasts (8, 17, 21, 36–38).

Toc159 is present in the cytosol as well as at the membrane (31). Although the function of this protein in the cytosol has not been clearly defined, a role for Toc159 as a cytosolic receptor that shuttles from the cytosol to chloroplasts has been proposed

(31). In this study we demonstrate that, in contrast to atToc159, the M domain is present only in the envelope membrane, and not in the cytosol. Clearly, atToc159M is sufficient to support protein import into chloroplasts in *ppi2* protoplasts, indicating that the absence of cytosolic atToc159 is not a problem for this process. However, in transgenic plants, the M domain is not sufficient for full complementation as determined by the degree of chloroplast biogenesis. Therefore, the possibility remains that the absence of atToc159 in the cytosol may affect chloroplast biogenesis in some unknown way.

In conclusion, we have demonstrated that the M domain is sufficient to direct the protein to the envelope membrane of chloroplasts, and to support protein import into chloroplasts and chloroplast biogenesis in the absence of atToc159. In addition, we propose that the G domain plays a regulatory role in the targeting of atToc159 to chloroplasts or support the function of atToc159 in the cytosol.

REFERENCES

1. Smeekens, S., Bauerle, C., Hageman, J., Keegstra, K., and Weisbeek, P. (1986) *Cell* **46**, 365–375
2. Hand, J. M., Szabo, L. J., Vasconcelos, A. C., and Cashmore, A. R. (1989) *EMBO J.* **8**, 3195–3206
3. Ko, K., and Cashmore, A. R. (1989) *EMBO J.* **8**, 3187–3194
4. Serra, E. C., Krapp, A. R., Ottado, J., Feldman, M. F., Ceccarelli, E. A., and Carrillo, N. (1995) *J. Biol. Chem.* **270**, 19930–19935
5. Rensink, W. A., Pilon, M., and Weisbeek, P. (1998) *Plant Physiol.* **118**, 691–699
6. Chen, X., and Schnell, D. J. (1999) *Trends Cell Biol.* **9**, 222–227
7. Keegstra, K., and Froehlich, J. E. (1999) *Curr. Opin. Plant Biol.* **2**, 471–476
8. Bauer, J., Chen, K., Hiltbrunner, A., Wehrli, E., Eugster, M., Schnell, D., and Kessler, F. (2000) *Nature* **403**, 203–207
9. Hirsch, S., Muckel, E., Heemeyer, F., von Heijne, G., and Soll, J. (1993) *Science* **266**, 1989–1992
10. van't Hof, R., van Klompenburg, W., Pilon, M., Kozubek, A., de Korte-Kool, G., Demel, R. A., Weisbeek, P. J., and de Kruijff, B. (1993) *J. Biol. Chem.* **268**, 4037–4042
11. Bruce, B. D. (1998) *Plant Mol. Biol.* **38**, 223–246
12. van't Hof, R., and de Kruijff, B. (1995) *J. Biol. Chem.* **270**, 22368–22373
13. Schleiff, E., and Soll, J. (2000) *Planta* **211**, 449–456
14. Gavel, Y., and von Heijne, G. (1990) *FEBS Lett.* **261**, 455–458
15. Schnell, D. J., Kessler, F., and Blobel, G. (1994) *Science* **266**, 1007–1012
16. Hinnah, S. C., Wagner, R., Sveshnikova, N., Harrer, R., and Soll, J. (2002) *Biophys. J.* **83**, 899–911
17. Schleiff, E., Soll, J., Kuchler, M., Kuhlbrandt, W., and Harrer, R. (2003) *J. Cell Biol.* **160**, 541–551
18. Sohr, K., and Soll, J. (2000) *J. Cell Biol.* **148**, 1213–1221
19. Jarvis, P., Chen, L. J., Li, H., Peto, C. A., Fankhauser, C., and Chory, J. (1998) *Science* **282**, 100–103
20. Gutensohn, M., Schulz, B., Nicolay, P., and Flugge, U. I. (2000) *Plant J.* **23**, 771–783
21. Bauer, J., Hiltbrunner, A., Weibel, P., Vidi, P. A., Alvarez-Huerta, M., Smith, M. D., Schnell, D. J., and Kessler, F. (2002) *J. Cell Biol.* **159**, 845–854
22. Smith, M. D., Hiltbrunner, A., Kessler, F., and Schnell, D. J. (2002) *J. Cell Biol.* **159**, 833–843
23. Jarvis, P., and Soll, J. (2000) *Biochim. Biophys. Acta* **1541**, 64–79
24. Clough, S. J., and Bent, A. F. (1998) *Plant J.* **16**, 735–743
25. Jin, J. B., Kim, Y. A., Kim, S. J., Lee, S. H., Kim, D. H., Cheong, G. W., and Hwang, I. (2001) *Plant Cell* **13**, 1511–1526
26. Kim, Y.-W., Park, D. S., Park, S. C., Kim, S. H., Cheong, G. W., and Hwang, I. (2001) *Plant Physiol.* **127**, 1243–1255
27. Lee, K. H., Kim, D. H., Lee, S. W., Kim, Z. H., and Hwang, I. (2002) *Mol. Cell* **14**, 388–397
28. Sohn, E. J., Kim, E. S., Zhao, M., Kim, S. J., Kim, H., Kim, Y.-W., Lee, Y. J., Hillmer, S., Sohn, U., Jiang, L., Hwang, I. (2003) *Plant Cell* **15**, 1057–1070
29. Hiltbrunner, A., Bauer, J., Vidi, P. A., Infanger, S., Weibel, P., Hohwy, M., and Kessler, F. (2001) *J. Cell Biol.* **154**, 309–316
30. Lee, Y. J., D. H. Kim, Kim, Y.-W., and Hwang, I. (2001) *Plant Cell* **13**, 2175–2190
31. Niwa, Y., Hirano, T., Yoshimoto, K., Shimizu, M., and Kobayashi, H. (1999) *Plant J.* **18**, 455–463
32. Downward J. (1990) *Trends Biochem. Sci.* **15**, 469–472
33. Sheen, J. (2001) *Plant Physiol.* **127**, 1466–1475
34. Bauer, J., Hiltbrunner, A., and Kessler, F. (2001) *Cell Mol. Life Sci.* **58**, 420–433
35. Surpin, M., Larkin, R. M., and Chory, J. (2002) *Plant Cell* **14**, 327–338
36. Kessler, F., Blobel, G., Patel, H. A., and Schnell, D. J. (1994) *Science* **266**, 1035–1039
37. Seedorf, M., Waegemann, K., and Soll, J. (1995) *Plant J.* **7**, 401–411
38. Kouranov, A., and Schnell, D. J. (1997) *J. Cell Biol.* **139**, 1677–1685